Moderate Ce Doping Enables Outstanding Oxygen Evolution Activity and Stability in CoMn-LDH Nanosheets

Wenjie Cao[a,b,‡], Yangchun Guo[a,b‡], Kuan Wang[b,*], Yuhao Zhou[a], Xuan Zhao[a,b], Yinfeng Wang[a,b], Zhenhong He[b], Shufang Ma[a], Bingshe Xu[a,c], Xiaodong Hao[a,*]

[a]*Xi'an Key Laboratory of Compound Semiconductor Materials and Devices, School of Physics & Information Science, Shaanxi University of Science & Technology, Xi'an 710021, China*

[b]*Shaanxi Key Laboratory of Chemical Additives for Industry, College of Chemistry and Chemical Engineering, Shaanxi University of Science & Technology, Xi'an 710021, China*

[c]*Key Laboratory of Interface Science and Engineering in Advanced Materials, Ministry of Education, Taiyuan University of Technology, Taiyuan, 030024, China*

*Corresponding author: E-mail: (X. Hao) hao.xiaodong@sust.edu.cn; (Kuan Wang) wangkuan@sust.edu.cn;

‡W. Cao and Y. Guo contributed equally to this work.

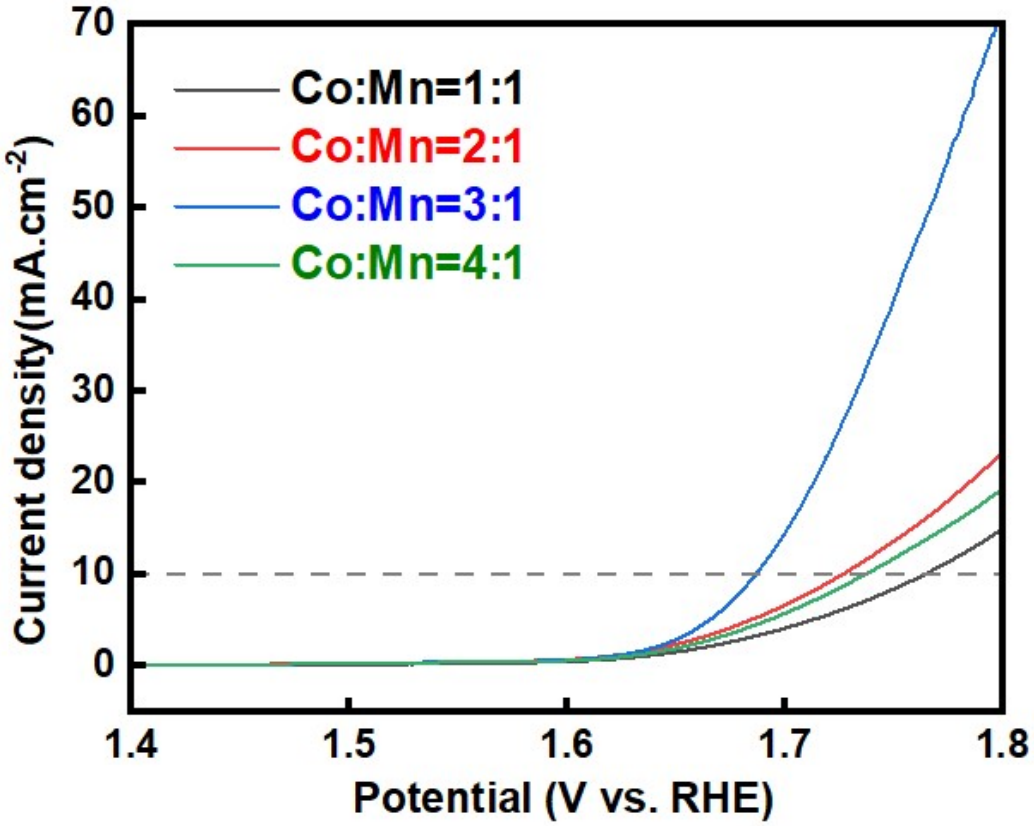

Fig. S1 Effect of different Co/Mn molar ratios on the OER catalytic performance of CM-LDH catalysts and determination of the optimal ratio

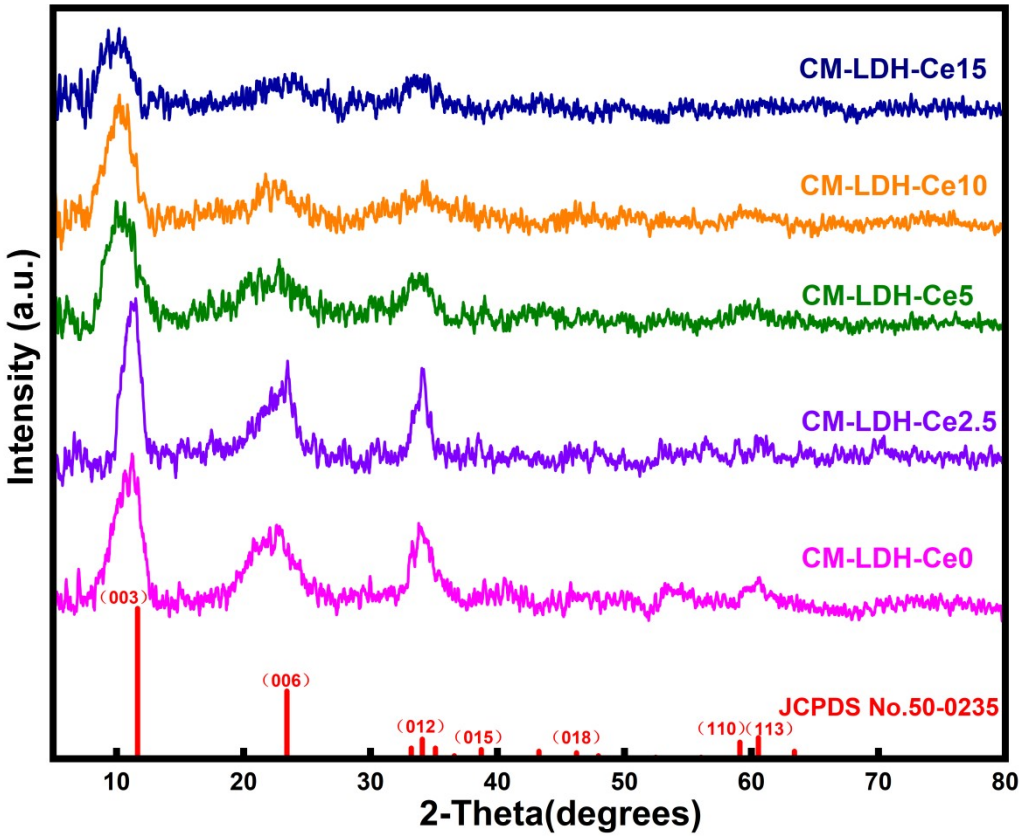

Fig. S2 XRD patterns of CM-LDH-Ce with different Ce doping ratios (0%, 2.5%, 5%, 10%, 15%).

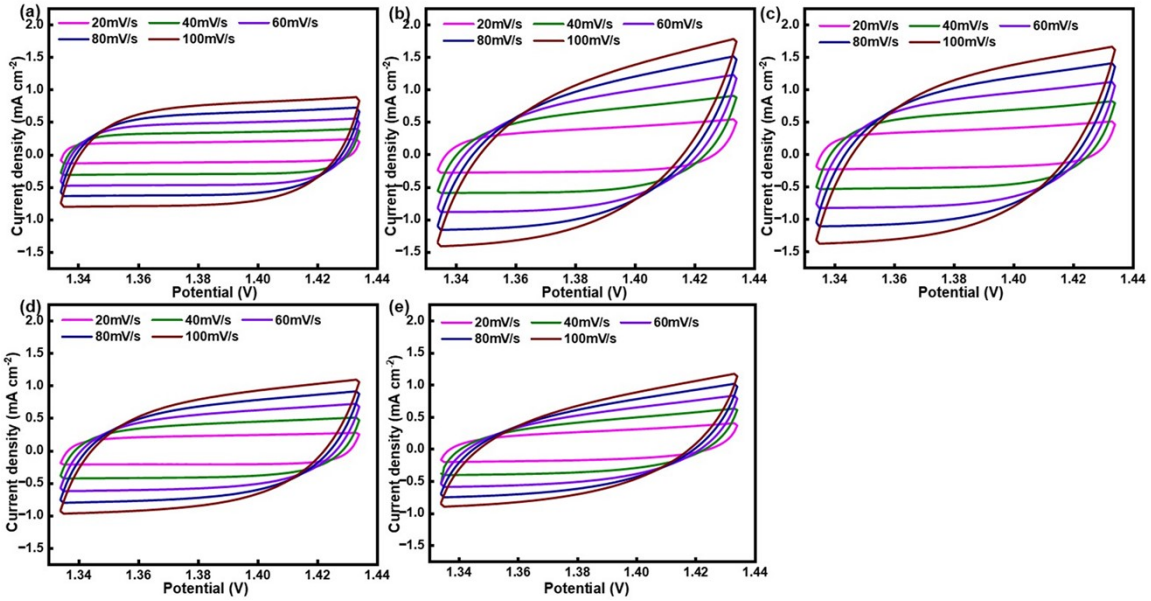

Fig. S3 Cyclic Voltammetry (CV) Curves and Electrochemical Reversibility Analysis of CM-LDH-Ce Catalysts with Different Ce Doping Contents

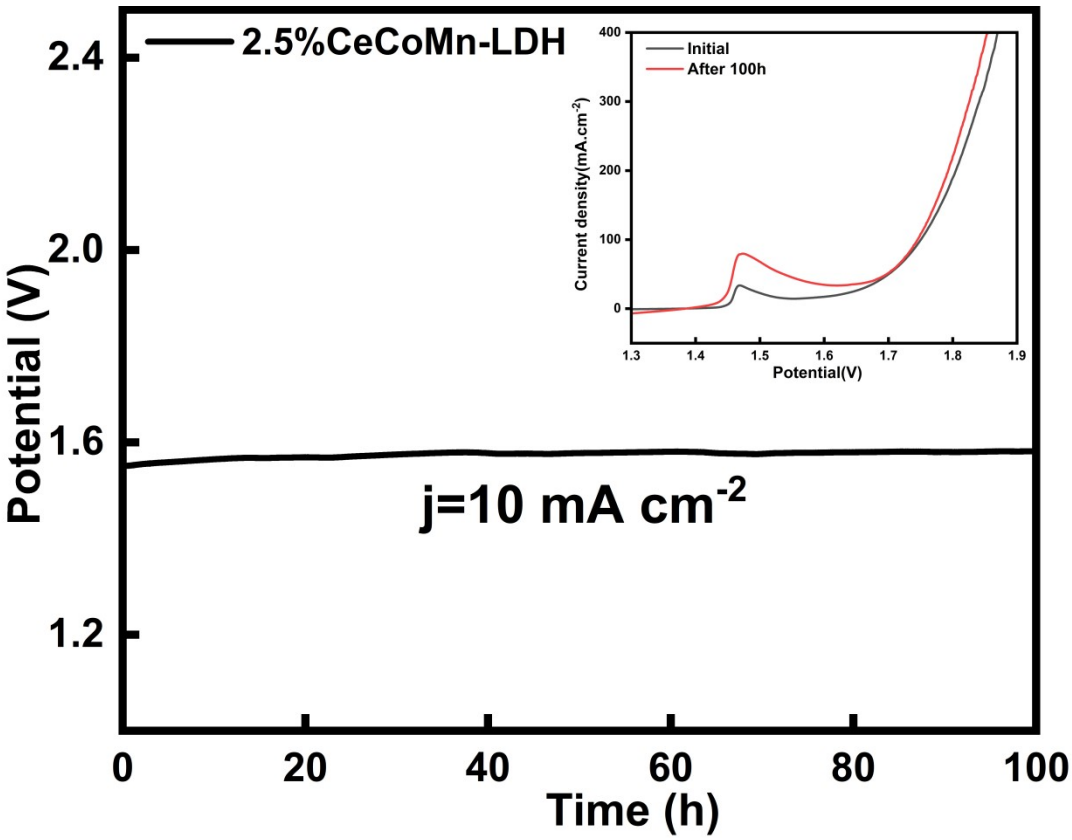

Fig. S4 Stability curve of CM-LDH-Ce2.5 at a current density of 10 mA cm^{-2}

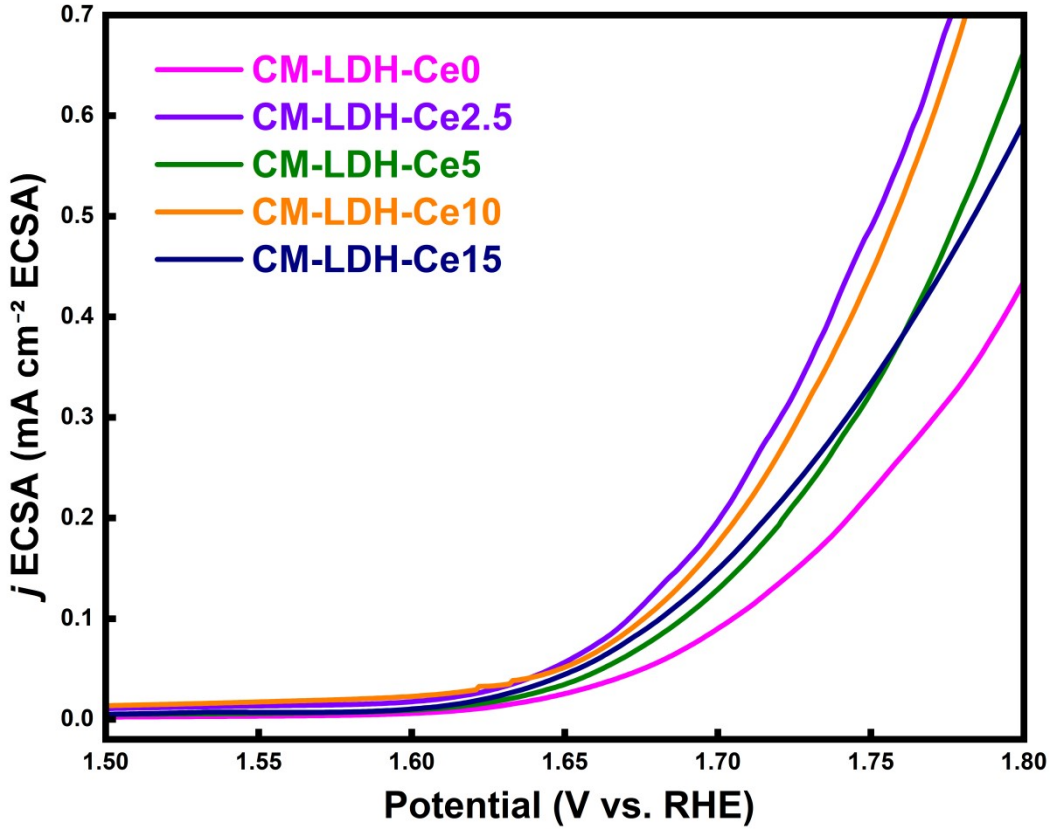

Fig. S5 ECSA-normalized LSV curves of CM-LDH-Ce catalysts.

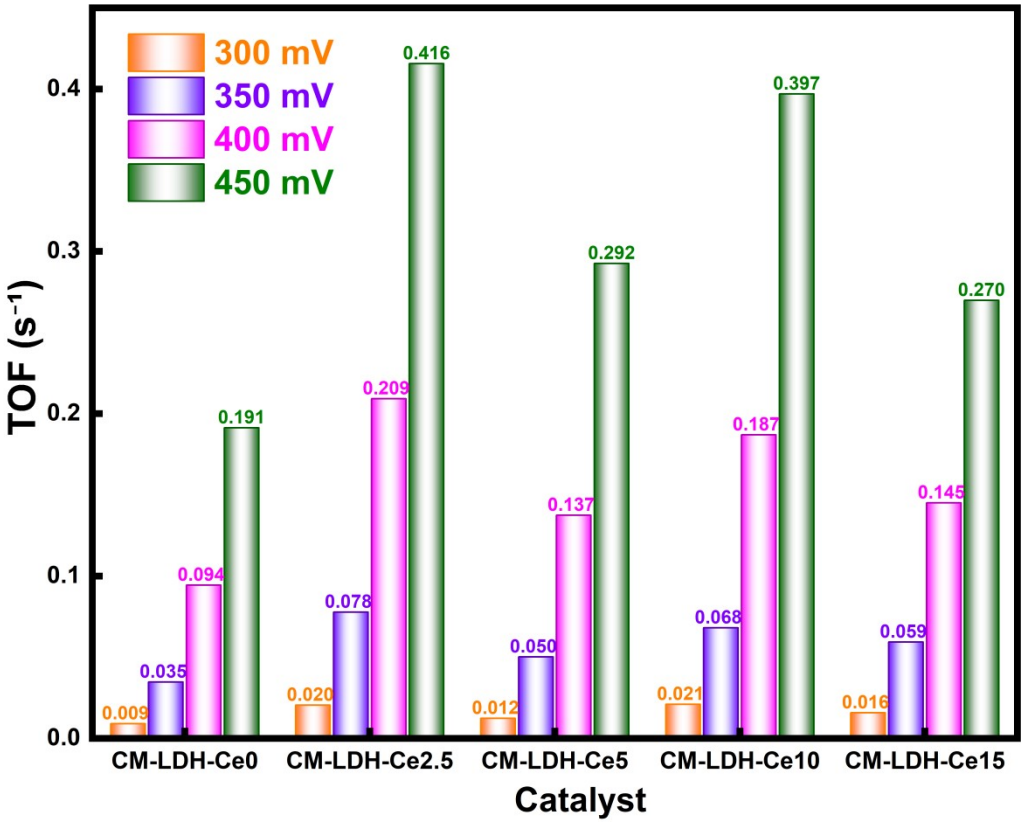

Fig. S6 Bar Chart Showing Turnover Frequency (TOF, s^{-1}) Values for CM-LDH-Ce Catalysts with Varying Ce Doping Contents, Measured at Fixed Overpotentials of 300, 350, 400, and 450 mV.

Table S1 XPS Valence State Peak Area Percentages of CM-LDH-Ce Catalysts with Different Ce Doping Contents.

	Proportion of Co peak area %		Proportion of Mn peak area %		Proportion of O peak area %			Proportion of Ce peak area %	
	Co^{2+}	Co^{3+}	Mn^{2+}	Mn^{3+}	H-O	OH^-	V_O	Ce^{3+}	Ce^{4+}
CM-LDH-Ce0	46.03	53.98	49.13	50.87	2.30	90.15	7.55		
CM-LDH-Ce2.5	56.70	43.30	49.59	50.41	2.11	89.68	8.21	22.96	77.03
CM-LDH-Ce5	61.52	38.48	44.42	55.58	1.56	89.56	8.88	20.54	79.45

Table S2 XPS Valence State Percentages of CM-LDH-Ce Catalysts with Different Ce Doping Contents.

	Valence state ratio of Co (Co^{2+}/Co^{3+})	Valence state ratio of Mn (Mn^{2+}/Mn^{3+})	Valence state ratio of Ce (Ce^{3+}/Ce^{4+})
CM-LDH-Ce0	0.85	0.97	
CM-LDH-Ce2.5	1.31	0.98	0.30
CM-LDH-Ce5	1.59	0.80	0.26

Table S3 Table of Original EPR Peak Areas and Relative Oxygen Vacancy Contents of CM-LDH-Ce Catalysts with Different Ce Doping Contents.

Ce doping content (%)	Original EPR peak area (a.u.)	Relative oxygen vacancy content (taking 0% Ce as 1)
0	4.23631×10^{-4}	1.00
2.5	5.8696×10^{-4}	1.38
5	7.50053×10^{-4}	1.77

Table S4 Comprehensive comparison of OER performance of recently reported doped/activated LDH-based electrocatalysts in alkaline media (including additional catalysts and detailed metrics).

Catalyst	LDH host	Strategy	Conc. levels	Substrate	η_{10} (mV)	η_{500} (mV)	Tafel (mV dec^{-1})	Stability (h)
CM-LDH-Ce2.5 (This work)	**CoMn**	**Ce doping**	**5**	**GCE**	**287**	**500**	**87.12**	**200 h @ 100 mA cm^{-2}**
N@CoMn-LDH/CC[1]	CoMn	N_2 plasma	2	CC	219	–	39.6	>50 h @ 100 mA cm^{-2}
V_{Mn}-MnCo-LDH/NF[2]	MnCo	Mn vacancy	7[a]	NF	253	–	38.63	120 h @ 50 mA cm^{-2}
Ce-NiFe LDH/NF[3]	NiFe	Ce doping	2	NF	–[b]	268	60.25	250 h @ 1 A cm^{-2} 500 h @ 1 A cm^{-2} [c]
Ce@CoFe-LDH[4]	CoFe	Ce doping + interface	2	NF	207	–	50.0	120 h @ 100 mA cm^{-2}
Ce-CoFe-LDH/NF[5]	CoFe	Ce doping	2	NF	225	–	34.34	24 h @ 50 mA cm^{-2}
CeLa-CoNiFe-LDH[6]	CoNiFe	Ce+La co-doping	2	NF	175	424	–	120h @ 10 mA cm^{-2}
$CoFe_{0.75}Mn_{0.25}$-LDH[7]	CoFe	Mn ternary	4[a]	NF	225[d]	–	133.0[e]	30 h @ 50 mA cm^{-2}
$ZnCo_2O_4$@NiCo-LDH[8]	NiCo	Interface eng.	–	NF	296.1	–	24.13	12 h @ 10 mA cm^{-2}

[a] Precursor molar ratio variation, not doping concentration levels.

[b] η_{10} not individually reported; the original paper focuses on ampere-level current densities (η at 1 A cm^{-2} = 324 mV in 1 M KOH; η at 1 A cm^{-2} = 390 mV in 1 M KOH + seawater).

[c] 250 h measured in 1 M KOH at 1 A cm^{-2}; 500 h measured in 1 M KOH + seawater at 1 A cm^{-2}.

[d] Reported as η_{20} in the original paper; η_{10} value is approximately 225 mV.

[e] Tafel slope calculated at 100 mA cm^{-2}.

GCE = glassy carbon electrode (drop-cast); NF = nickel foam (self-supported); CC = carbon cloth (self-supported). All data measured in 1.0 M KOH unless otherwise specified. "–" indicates the value was not reported in the original paper.

References

1 L. Yang, Q. Lin, D. Guo, L. Wu, Z. Guan, H. Jin, G. Fang, X. a. Chen and S. Wang, *Inorg. Chem.,* 2023, **62**, 17565–17574.

2 B. Li, L. Dai, G. Su, Z. Xia, Y. Ye and Z. Li, *Fuel,* 2024, **364**, 130961.

3 Y. Yao, S. Sun, H. Zhang, Z. Li, C. Yang, Z. Cai, X. He, K. Dong, Y. Luo, Y. Wang, Y. Ren, Q. Liu, D. Zheng, W. Zhuang, B. Tang, X. Sun and W. Hu, *J. Energy Chem.,* 2024, **91**, 306–312.

4 X. Sun, R. Wang, Q. Wang and K. Ostrikov, *Inorg. Chem. Front.,* 2024, **11**, 1458–1471.

5 N. Wang, X. Wang, Y. Shan, J. Liu, J. Zhang, K. Chen and X. Yu, *React. Chem. Eng.,* 2023, **8**, 2746–2756.

6 R. R. K. P., P. Wang, M. He, S. Meng, J. Yao, H. Li, C. Yang and Z. Li, *Sci. China Chem.,* 2024, **67**, 2586–2598.

7 Y. Zheng, K. Sun, J. Pang, J. Hou, G. Wang, W. Guo, L. Wang, X. Guo and L. Chen, *J. Alloys Compd.,* 2022, **925**, 166754.

8 R.-Y. Li, S.-L. Xu, Z.-Q. Ai, J.-G. Qi, F.-F. Wu, R.-D. Zhao and D.-P. Zhao, *Int. J. Hydrogen Energy,* 2024, **91**, 867–876.